Journal of Science and Technology in Civil Engineering, NUCE 2020. 14 (3): 26–39

MODELING THE FLEXURAL BEHAVIOR OF CORRODED REINFORCED CONCRETE BEAMS WITH CONSIDERING STIRRUPS CORROSION

Nguyen Trung Kien[a], Nguyen Ngoc Tan[a,*]

[a] *Faculty of Building and Industrial Construction, National University of Civil Engineering, 55 Giai Phong street, Hai Ba Trung district, Hanoi, Vietnam*

Article history:
Received 22/05/2020, Revised 14/07/2020, Accepted 21/07/2020

Abstract

The reinforcement corrosion is one of the most dominant deterioration mechanisms of existing reinforced concrete structures. In this paper, the effects of the stirrup corrosion on the structural performance of five corroded beams have been simulated using the finite element model with DIANA software. These tested beams are divided into two groups to consider different inputs: (i) without corroded stirrups in flexural span, (ii) with locally corroded stirrups at different locations (e.g. full span, shear span, middle span). FE model has been calibrated with experimental results that were obtained from the four-point bending test carried out on the tested beams. This study shows that the stirrups corrosion should receive more attention in the serviceability limit state due to its considerable effect on flexural behavior. Based on a parametric study, it shows that the effect of the cross-section loss of tension reinforcements on the load-carrying capacity of the corroded beam is more significant than the bond strength reduction.

Keywords: reinforced concrete; beam; stirrup corrosion; finite element model; flexural nonlinear behavior.

https://doi.org/10.31814/stce.nuce2020-14(3)-03

1. Introduction

The corrosion of reinforcement is one of the most dominant deterioration mechanisms of reinforced concrete (RC) structures. It inflicts damages which lead to a decrease in the performance as well as safety of RC structures [1]. The corrosion of steel rebars is associated with the loss of cross-section, the propagation of the concrete crack, and the reduction of bond strength between steel and concrete. They lead to complex distributions of strains and stresses, highly nonlinear, path-dependent behavior. In fact, many studies were conducted by both experimental and theoretical methods on corroded RC beams. For example, the effect of the spatial variability of steel corrosion on the structural performances of corroded RC beams has been experimentally investigated and discussed by Lim et al. [1]. It concluded that if the non-uniform steel weight loss along the steel rebar is adequately assessed, the local damages of corroded RC beams can be physically captured. For a low dispersion of cross-section loss, the structural capacity of the corroded beam is governed by the corrosion levels. As the dispersion of the steel cross-section loss raises, the pitting corrosion or the local variability of the steel cross-section loss has a more significant impact than the corrosion level. Coronelli and Gambarova [2] studied the modeling of corroded RC beams. It stated that a critical aspect is an assessment

*Corresponding author. *E-mail address:* tannn@nuce.edu.vn (Tan, N. N.)

of pitting corrosion in the finite element (FE) model, which may induce brittle behavior in the steel rebars. Therefore, corrosion affects both the strength and the ductility of a structure. In order to assess the serviceability of a corroded RC structure, the parameters should be taken into consideration are not only concrete cover depth and steel rebar cross-section loss but also the reduction of the concrete section. A two-dimensional nonlinear FE model has been developed in the study of Kallias et al. [3] to assess the structural performance of a series of RC beams damaged by ranging corrosion levels at different locations. This study shows that the loss of steel cross-section and associated concrete damage/section loss (due to the accumulation of expansive corrosion products) are found to be the main causes of loss of strength and bending stiffness. The bond deterioration is responsible for changes in cracking patterns and widths. Consequently, modeling bond deterioration is highly significant for performance assessment at the serviceability limit state. The study of Sæther et al. [4] had been conducted on how to the use of FE analysis to simulate the mechanical response of RC structures with corroded reinforcement.

In Vietnam, although the major deterioration of coastal structures is related to corrosion of steel reinforcement [5], the number of research works that are related to this subject is still limited. Previous studies have been conducted mainly by surveying and statistical methods to assess the extent and damage of corrosion, but have not yet produced results on the behavior of corroded structures. In recent years, several research works have been firstly performed to assess the behavior of corroded RC structures in a chloride environment. Tan and Hiep [6] analyzed the potential of existing empirical models for prediction of steel corrosion rate by using a series of experimental data collected from the literature. In an experimental study on the influence of reinforcement corrosion on steel - concrete bond stress by Tan et al. [7], it concluded that when the corrosion level was in the range of 0 to 2%, the bond stress between corroded steel and concrete is larger than that of uncorroded reinforcement and concrete. As the corrosion level increases to 6.5% and more than 8.4%, the bond stress of corroded RC components decreases from 30% to 62% compared with the uncorroded case. Nguyen and Tan [8] conducted a study on the prediction of the residual carrying capacity of the RC column subjected in-plane axial load considering corroded longitudinal steel rebars using the finite element method. This study concluded that the residual carrying capacity of corroded RC column is governed by the location and corrosion level of reinforcement. The corrosion of longitudinal steel rebars in the tension zone of the column results in a more significant impact on the reduction of carrying capacity compared with the case of corroded rebars in the compression zone.

Recently, the studies consider mainly the influence of corroded longitudinal reinforcement on the flexural behavior of RC beams, but there are only a few that mention how stirrups corrosion affects structural behavior. In this study, to understand the flexural capacity of RC beam with stirrups corrosion, several corroded beams have been simulated to examine the suitable constitutive model using FE analysis in DIANA software. The simulation was carried out on five tested RC beams that are divided into two cases: (i) without corroded stirrups in flexural span (only U-type stirrups at middle span); (ii) with corroded stirrups at different locations and of different corrosion levels. The validation of the simulation has been based on the load – deflection relationship that is calibrated by the experimental data. The simulation results can represent the flexural behavior (e.g. load carrying capacity, deflection) of the tested beams. Moreover, a parametric study was also realized to assess the effect of the bond strength reduction and the cross-section loss of corroded steel rebars on the flexural behavior of corroded beams.

2. Materials law for modeling corroded RC beam

2.1. Concrete material law

The expansion of corrosion products induces the crack and spalling of concrete. Consequently, the concrete area that is degraded by corrosion damage-induced reduced strength compared to that of the undamaged concrete areas. The corrosion damage on the concrete cover is considered in the FE model by modifying the stress-strain relationship of the concrete, as suggested by Lim et al. [1] as illustrated in Fig. 1.

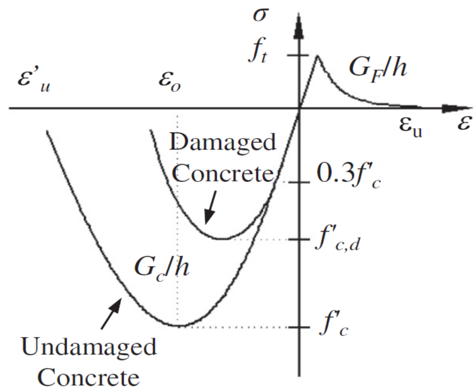

Figure 1. Constitutive law of concrete in compression and tension [1]

The deterioration of the concrete compressive strength can be described by Eq. (1) with $f'_{c,d}$ being the compressive strength of the corroded concrete, f'_c being the compressive strength of the non-corroded concrete, k' being the coefficient related to bar roughness and diameter, for the case of medium-diameter ribbed rebars a value $k' = 0.1$ has been proposed by Cape [9], ε_0 being the strain at the compressive strength f'_c, and ε_1 being the average smeared tensile strain in the transverse direction.

$$f'_{c,d} = f'_c / \left[1 + k' \left(\varepsilon_1/\varepsilon_0\right)\right] \tag{1}$$

The strain ε_1 can be estimated by Eq. (2) with b_0 being the section width in the state without corrosion crack, b_f being the beam width expanded by corrosion cracking.

$$\varepsilon_1 = \left(b_f - b_0\right)/b_0 \tag{2}$$

$$b_f - b_0 = n_{bars} w_{cr} \tag{3}$$

where n_{bars} is the number of rebars; and w_{cr} is the total crack width at a given corrosion level. The total crack width w_{cr} can be determined as Eq. (4) proposed by Molina et al. [10].

$$w_{cr} = 2\left(v_{rs} - 1\right) X_d \tag{4}$$

where v_{rs} is the ratio between the specific volumes of rust and steel that can be assumed to be 2 [10]. X_d is the depth of the penetration attack that is determined by Eq. (5) proposed in the study of Val [11], with i_{corr} (μA/m^2) being the corrosion current density in the steel bar and t (years) being the duration of corrosion.

$$X_d = 0.0116 i_{corr} t \tag{5}$$

2.2. Steel reinforcement law

Previous studies reported that both strength and ductility corroded reinforcement are affected mainly due to variability in steel cross-section loss over their lengths [12]. Because of the difficulty in implementing the actual variability of steel corrosion in the numerical model, an alternative approach is suggested by modeling the corroded steel rebar over a length based on average cross-section loss together with empirical coefficients. The use of empirical coefficients (whose values are smaller than 1) is to account for the reduction in strength and ductility of corroded rebar attributed to the irregular cross-section loss along the rebar length in addition to the reduction attributed to the average cross-section. Since the corrosion damage on the rebar is considered in the FE model by reducing the steel cross-sectional areas over the rebar length according to steel weight loss, the simplified bilinear constitutive stress - strain relationship of steel as illustrated in Fig. 2 is used without empirical coefficients, where the post-yield modulus is assumed to be 1% of its elastic modulus E_s. Where, f_y and f_{su} are the yield tensile strength and ultimate tensile strength of steel. ε_y and ε_{su} are the yield strain and maximum strain of steel, respectively.

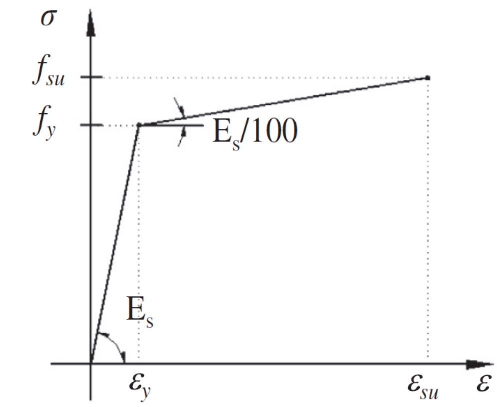

Figure 2. Stress - strain relationship of the steel reinforcement [1]

2.3. *Model of steel – concrete deteriorated bond*

The two significant factors that have huge effects on the bond stress - slip relationship are the amount of steel corrosion and the confinement of the concrete. There is a consensus on its well-defined trend that the bond strength initially increased with the corrosion amount in the pre-cracking stage and then substantially decreased as the longitudinal corrosion cracking developed along with the steel reinforcement [1]. However, bond failure in corroded rebars is mostly by splitting, for the commonly used concrete covers and stirrup amounts. Consequently, the parameters of the bond - stress relationship must be modified to reproduce such brittle behavior. Therefore, the residual bond stress - slip curve as proposed by Kallias and Rafiq [3] is used herein for the deteriorated bond between steel and concrete as illustrated in Fig. 3. For the non-corroded steel bar, the good bond between steel and concrete is illustrated by stress - slip curve in CEB-FIP [13].

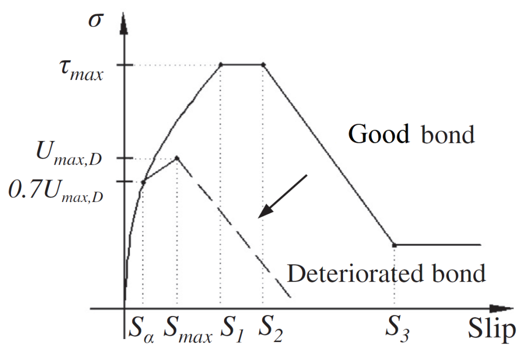

Figure 3. Constitutive law of the deteriorated bond [1]

The residual bond - slip relationship can be described as the following Eqs. (6), (7) and (8).

$$U = U_1 (S/S_1)^{0.3} \tag{6}$$

$$S_\alpha = S_1 (\alpha' U_{\max,D}/U_1)^{1/0.3} \tag{7}$$

$$S_{\max} = S_1 \exp[(1/0.3)\,\mathrm{Ln}(U_{\max,D}/U_1)] + S_0\,\mathrm{Ln}(U_1/U_{\max,D}) \tag{8}$$

where $\alpha' = 0.7$; $U_1 = 2.57 (f'_c)^{0.5}$ with f'_c is the compressive strength of non-corroded concrete; $S_1 = 0.15c_0$ with $c_0 = 8.9$ mm that is the spacing between the ribs of the steel bar; $S_2 = 0.35c_0$; and

S_0 = 0.15 or 0.4 mm for plain concrete or steel confined concrete, respectively.

$$U_{\max,D} = R\left[0.55 + 0.24\left(c/d_b\right)\right] + 0.191\left(A_{st}f_{yt}/S_s d_b\right) \tag{9}$$

$$R = A_1 + A_2 m_L \tag{10}$$

The residual bond strength $U_{\max,D}$ can be determined by Eq. (9), with c is the concrete cover, d_b is the diameter of the longitudinal rebar, A_{st} is the cross-section area of the stirrup, f_{yt} is the yield strength of the stirrup, S_s is the stirrup spacing. R is the factor accountable for the residual contribution of concrete towards the bond strength as a function of $A_1 = 0.861$ and $A_2 = 0.014$, which is related to the current density used in the accelerated corrosion test, and m_L is the amount of steel weight loss in percentage (Eq. (10)). Eq. (9) consists of two separate terms: the first and second terms are attributed to the concrete and stirrup contributions to the bond strength, respectively. The effectiveness of this equation is that the level of confinement can be varied with the changes in the stirrup spacing and concrete compressive strength for different specimens.

3. Validation of FE models for flexural corroded RC beams

3.1. Corroded beams without corroded stirrups in flexural span

a. Presentation of the tested beams by Dong et al. [14]

In this section, two RC beams with the dimensions of 1200 × 250 × 180 mm as illustrated in Fig. 4 from an experimental study conducted by Dong et al. [14] are used for modeling the corroded beams with U-type stirrups in the flexural span. These beams were tested to investigate the crack propagation and flexural behavior of RC beams under steel corrosion and sustained loading simultaneously. The stirrups were only places in the shear zones of the beams. Both the stirrups and tension reinforcements were corroded in the laboratory.

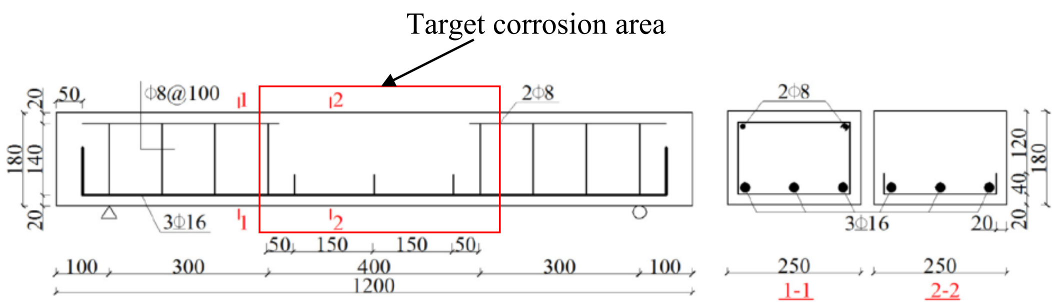

Figure 4. Layout and cross-sections of tested beams [14]

The tested beams were made of concrete having a 28-day compressive strength of 35.4 MPa. The reinforcements consisted of HRB335 steel rebars for tension longitudinal reinforcement, HPB300 plain steel rebars for compression longitudinal reinforcement and stirrups. The mechanical properties of these reinforcements are shown in Table 1, characterized by the nominal diameter, yield tensile strength, ultimate tensile strength, and elastic modulus.

In this study, three tested beams named FNN00, FCL03and FCL06 have been used to analyze and simulate the flexural behavior using the FE model. FNN00 was a non-corroded beam considered as the control beam. FCL03 and FCL06 were corroded for the target area in the flexural span (Fig. 4), which were simultaneously subjected to a sustained load corresponding to 30% and 60% of the expected ultimate load, respectively. After the failure of the tested beams with a four-point bending test, the corrosion levels of tension reinforcements and stirrups were determined by weighting the remaining mass of each steel rebar compared to the initial mass before corrosion. Table 2 presents the actual corrosion levels of reinforcements for these beams. It shows that the tension reinforcements were corroded at low levels of 2 to 3% on average, meanwhile, the stirrups were corroded at moderate levels of 11 to 12% on average. Table 3 presents the applied load and deflection of three tested beams, which are characterized by the load corresponding to yield strength of tension reinforcement (F_y, kN), the ultimate load at the failure (F_u, kN), the deflections at the mid-span of the tested beam denoted s_f and s_u corresponding to F_y and F_u.

Table 1. Mechanical properties of steel rebars

Rebar type	Nominal diameter (mm)	Yield strength (MPa)	Ultimate strength (MPa)	Elastic modulus (MPa)
HRB335	16	380.5	552.7	1.92×10^5
HPB300	8	396.9	535.7	$1.98x10^5$

Table 2. Corrosion levels of reinforcements in the tested beams

Tested beam	Corrosion level (%)		Failure mode
	Stirrup	Tension reinforcement	
FNN00	0	0	Flexural
FCL03	11.08	3.10	Flexural
FCL06	12.07	2.01	Flexural

Table 3. Experimental results of bending test on the tested beams by Dong et al. [14]

Tested beam	F_f (kN)	s_f (mm)	F_u (kN)	s_u (mm)	$s_u - s_f$ (mm)
FNN00	95.8	5.37	102.45	11.80	6.43
FCL03	92.1	3.90	100.30	9.25	4.90
FCL06	94.3	3.84	101.40	9.40	5.56

b. Modeling of the corroded beams without stirrups in flexural span

In this study, the concrete material has been modeled with an element mesh of $30 \times 3030 \times 30$ mm using a 20-node hexahedron solid element (CHX60 element in DIANA), while the slip reinforcements have been modeled as a three-node numerically integrated truss element (CL9TR element in DIANA) as illustrated in Fig. 5. A line-solid interface element has been used in order to simulate the influence of bond - slip behavior because it connects slip reinforcements to the continuum element in which the line element is located. Therefore, the interface elements based on the bond stress-slip relation from CEB-FIP 1990 [13] can be applied. In the part of the beam where there is no reinforcement, we assigned it as plain concrete with the same compressive strength as given in the previous section.

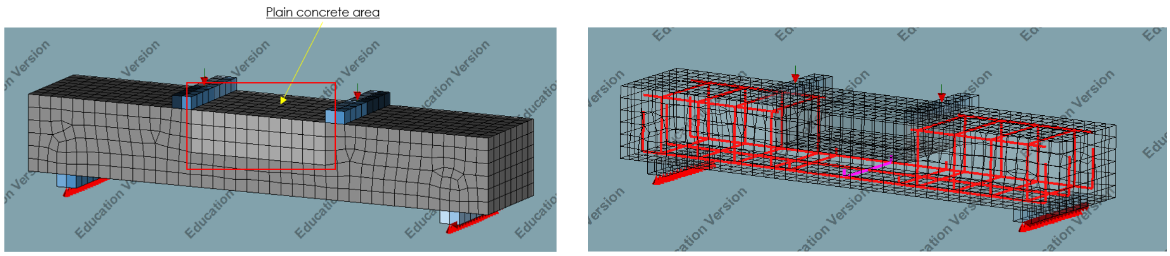

(a) Concrete mesh (b) Reinforcement mesh

Figure 5. Three-dimensional FE model of the corroded beams without stirrups in the flexural span

In this analysis, since there is no information for the spatial variability of corrosion for the stirrups and tension reinforcement, we have simulated the corroded steel rebar over a length based on average cross-section loss. In addition, the effect of corrosion is modeled by reducing the cross-section of the steel rebars based on the information given in Table 2 and modifying the constitutive law of damaged concrete, steel, and their interface (bond).

c. Validation of FE model

Fig. 6 shows good agreement between the experimental and numerical results for the load – deflection curves of two corroded beams FCL03 and FCL06. FE model can predict the ultimate flexural strength of tested beams with good accuracy. In fact, the applied loads corresponding to the yield tensile strength of steel reinforcement of the corroded beams FCL03 and FCL06 are equal to 92.1 kN and 94.3 kN, respectively. FEM results are about 1% to 2% different from the experimental results. Dong et al. [14] noted that since the corrosion levels of tension reinforcements in the tested beams were relatively low (2% to 3%), and thus there is a negligible difference in the ultimate loads between two corroded beams and control beam.

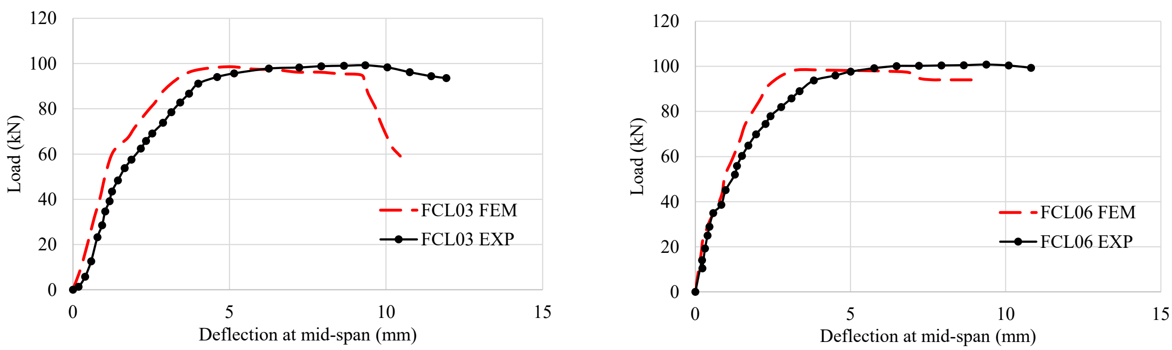

(a) Beam FCL03 (b) Beam FCL06

Figure 6. Load - deflection curves of corroded beams without stirrups by experiment and FEM analysis

For a target load, the estimated deflection by the FE model is slightly lower than the measured deflection by the test. This result can be explained that the simulated beam has lower ductility than the experimental beam since the non-reinforced area has been assigned with plain concrete. Meanwhile, the difference of the stiffness between the modeled and experimental beams can be ascribed to existing cracks due to corrosion before loading, which is hardly implemented in the simulation properly.

Moreover, at the end of the bending test, the failure of two corroded beams FCL03 and FCL06 was the flexural mode and similar to those of the control beam FNN00.

In addition, the cracks due to loading developed upwards from the bottom surface of the beam. In the flexural span of each corroded beam, these cracks were found to be typically in the vertical direction and parallel as illustrated in Fig. 7 (e.g. front, bottom, and back faces). Among these cracks, two or three major cracks with important width were experimentally identified in the cracking map, which can be represented by FE analysis.

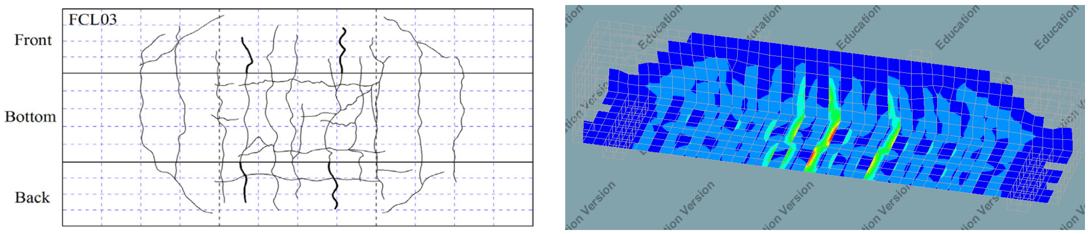

(a) Crack pattern on the beam FCL03 by experiment and numerical analysis

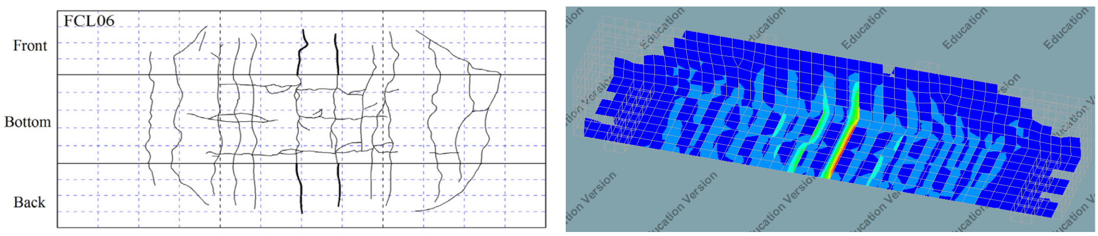

(b) Crack pattern on the beam FCL06 by experiment and numerical analysis

Figure 7. Comparison of the crack pattern on the corroded beam without stirrups using experiment and FEM

3.2. Corroded beams with locally corroded stirrups

a. Presentation of the tested beams by Ullah et al. [15]

In the section, three tested beams with the dimensions of 1800 × 100 × 150 mm in the study conducted by Ullah et al. [15] have been used for modeling the flexural beams with locally corroded stirrups. Fig. 8 presents the detail of these beams with numbering each stirrup and the diagram of the four-point bending test that was realized to assess their flexural behavior.

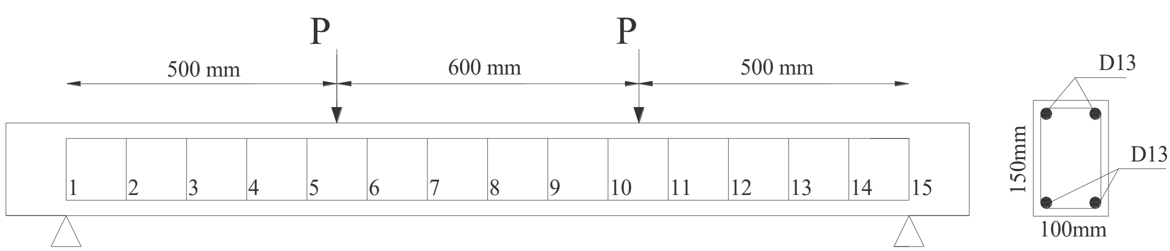

Figure 8. Layout and cross-section of tested beams [15]

The tested beams were made of concrete having the average compressive strength of 32 MPa. Longitudinal reinforcements were the steel rebars with a nominal diameter of 13 mm having the yield tensile strength of 395 MPa. In the other beams, while the longitudinal reinforcements were coated using epoxy resin to avoid corrosion, the stirrups in the tested beams composed of plain steel rebars with the nominal diameter of 6 mm having the yield tensile strength of 395 MPa.

In this study, four tested beams named B2-STD, B3-MC-FS, B7-MC-SS, B9-MC-MS have been used to analyze and simulate the flexural behavior using FE models. Beam B2-STD was a non-corroded beam considered as the control beam. In the other beams, while the longitudinal reinforcements were coated using epoxy resin to avoid corrosion, the stirrups were corroded at different locations in the tested beams, such as: (i) at the full span in beam B3-MC-FS, (ii) at the shear span in beam B7-MC-SS, and (iii) at the middle span in beam B9-MC-MS. Table 4 synthesized the experimental results of a four-point bending test on the tested beams. All tested beams were fractured by the flexural mode.

Table 4. Experimental results of bending test on the tested beams by Ullah et al. [15]

Beam name	Corrosion location	Peak load (kN)	Max. deflection (mm)	Failure mode
B2-STD	None	39.53	21.96	Flexural
B3-MC-FS	Full span	36.49	31.21	Flexural
B7-MC-SS	Shear span	37.03	21.89	Flexural
B9-MC-MS	Middle span	32.37	14.90	Flexural

After the failure of the corroded beams with a four-point bending test, the corrosion levels of stirrups were determined by weighting the remaining mass of each steel rebar compared to the initial mass before corrosion.

The corrosion levels were determined for each stirrup and presented in Fig. 9 for three corroded beams. For the simulation of corroded beams, an average corrosion level was calculated for all stirrups. Three corroded beams B3-MC-FS, B7-MC-SS and B9-MC-MS had the corrosion level of 7.2%, 10.5% and 11.6% on average, respectively. In particular, it notes that a stirrup (number 3) in the beam B7 was corroded with approximately 30% weight loss.

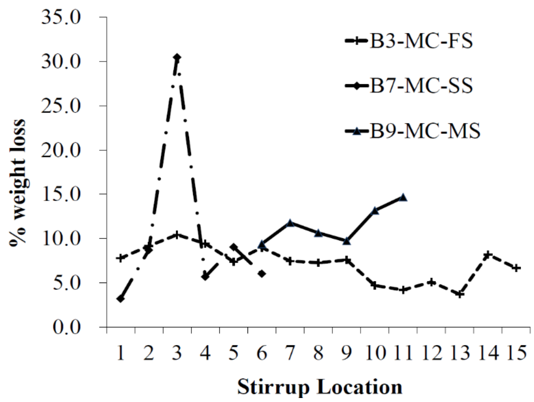

Figure 9. Corrosion profile of corroded stirrups in the tested beams [15]

b. Modeling of the flexural beams with locally corroded stirrups

A similar process as presented in paragraph 3.1.2 was performed for modeling the tested beams with corroded stirrups at different locations. The concrete material has been modeled with an element mesh of $30 \times 30 \times 30$ mm using a 20-node hexahedron solid element (CHX60 element), while the slip reinforcements are modeled as a three-node numerically integrated truss element (CL9TR element). The corroded steel rebar was simulated along the length based on an average cross-section loss. For each beam with locally corroded stirrups, the effects of corrosion in a target area were modeled by reducing the cross-section of the steel rebars and modifying the constitutive law of damage materials under corrosion, as well as the steel – concrete bond.

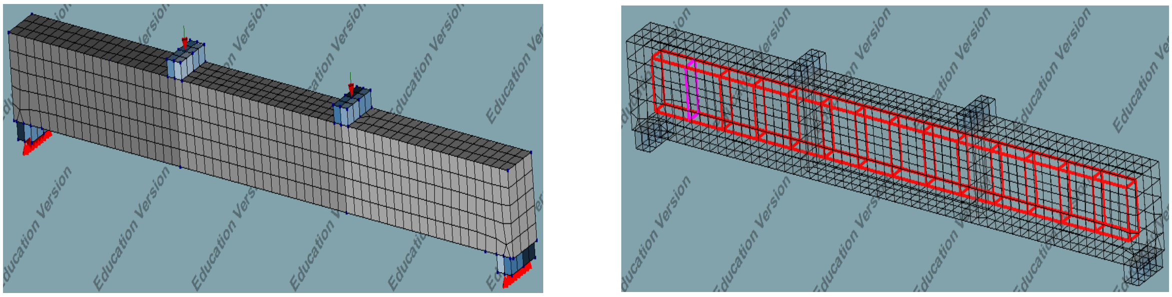

(a) Concrete mesh (b) Reinforcement mesh

Figure 10. Three-dimensional FE model of the corroded beams with locally corroded stirrups

c. Validation of the FE model

Fig. 11 shows acceptable agreement between experimental and tested results for the load-deflection curves of three beams with different locations of corroded stirrups. FE model can predict the ultimate flexural strength of tested beams with good accuracy. For mild corrosion (approximately 10% weight loss), the lowest flexural capacity was observed in the beam B9-MC-MS with an 18.11% reduction from the control beam, and corrosion of stirrups was done in a middle span. The maximum capacity of the beam B9 in the test was 32.4 kN compared with approximately 35.0 kN at the same deflection of FEM results. The beam B7-MC-SS with corroded stirrups in the shear span has the least reduction in load-carrying capacity (37.0 kN in test versus 39.0 kN in FEM). For the case of the beam B3-MC-FS, the reduction in flexural capacity was 7.69% compared with the control beam. The failure load of

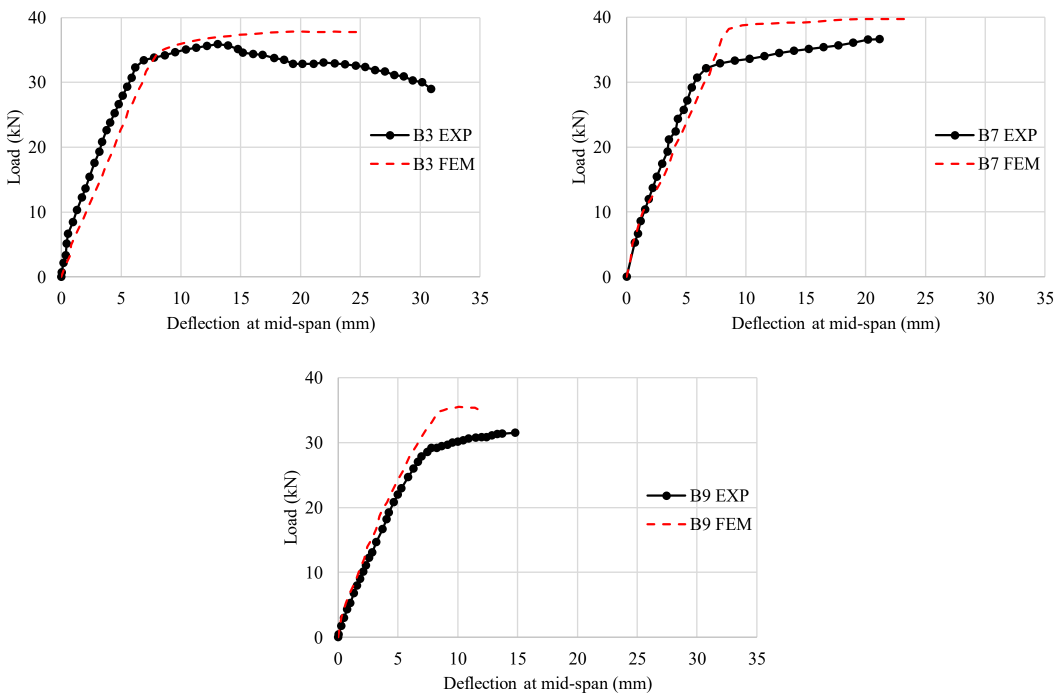

Figure 11. Load - deflection curves of tested beams with locally corroded stirrups using experiment and FEM

the beam B3 in FE analysis was 38 kN, which is 4% larger than the experimental result. In the case of flexural beams, stirrups that subjected to accelerated corrosion in the middle span have more effect on maximum capacity than in the shear span. However, the corrosion level of reinforcement affects the maximum capacity the most.

Additionally, the stiffness of the simulated beams is similar to those of the experimental beams throughout the evolution of damaging stages in both the pre- and post-peak regions. The ductility varied for all the corroded beams, as the location of the corrosion was not the same. Based on the deflection results, the beam B3-MC-FS showed the highest ductility, followed by B7-MC-SS as the stirrups were corroded in the shear span and B9-MC-MS shared the lowest ductility which can be obtained by using a numerical model.

In the case of the beam B3-MC-FS, which was corroded in the full span with 7.2% weight loss, many corrosion cracks were observed with the range of crack width from 0.05 to 0.25 mm [15]. The cracks due to loading at the failure stage are found concentrated in the middle span of the beam as illustrated in Fig. 12(a).

In the case of the beam B7-MC-SS, where the locations of corroded stirrups were in shear span, the cracks due to corrosion were found only in a part of the beam [15]. Fig. 12(b) shows that the spacing between cracks due to loading is larger than in the beam B3-MC-FS at the failure stage. Similarly, the corroded stirrups in the middle span in the case of the beam B9-MC-MS induced more cracks under loading and bigger spacing between them than the case of the beam B3-MC-FS.

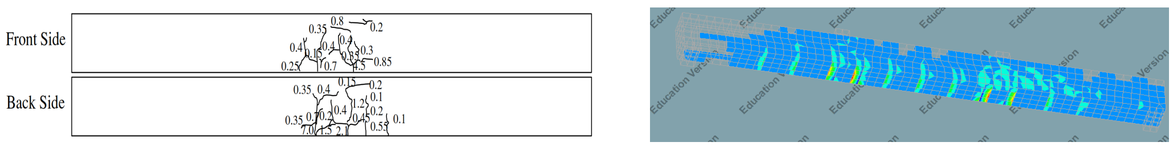

(a) Crack pattern of the beam B3 by experiment and numerical analysis

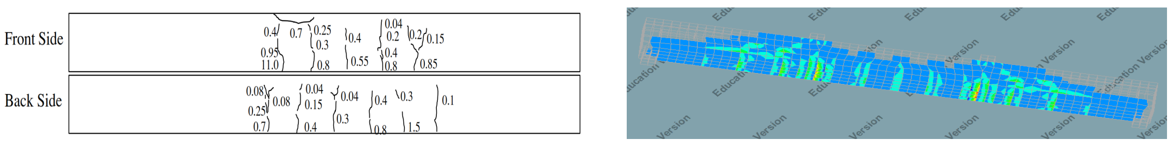

(b) Crack pattern of the beam B7 by experiment and numerical analysis

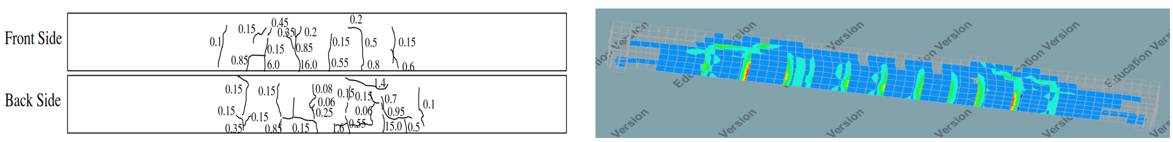

(c) Crack pattern of the beam B9 by experiment and numerical analysis

Figure 12. Comparison of crack pattern on the corroded beam with corroded stirrups using experiment and FEM

3.3. Parametric study on the flexural behavior of corroded beam

In this section, the tested beams have identical dimensions, material properties with the corroded beam FCL03 in the study of Dong et al. [14] (cf. section 3.1). Two parameters have been considered, which are the bond strength reduction and the cross-section loss of tension longitudinal reinforcements. Table 5 presents several cases for the bond strength reduction ranging from 0% to 80%, for the cross-section loss ranging from 10% to 50%. When either parameter is studied, other parameters are declared as the corroded beam FCL03.

Table 5. Parametric study for several bond strength reductions and cross-section losses

Beams index	Bond strength reduction (%)	Cross-section loss (%)
FCL03–0	0	0
FCL03–1	30	20
FCL03–2	50	30
FCL03–3	80	50

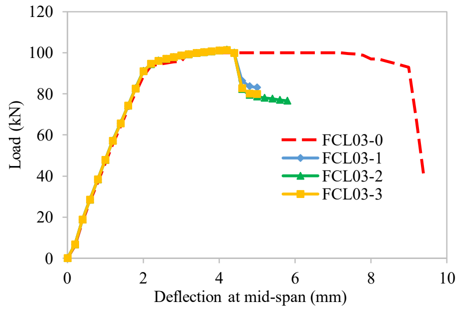

Figure 13. Load - deflection curves with several bond strength reductions

a. Effect of the bond strength reduction

The simulation results of the load – deflection curve are presented in Fig. 13 for assessing the effect of bond strength ranging from 0% to 80%. The results obtained show that the bond strength reduction has a negligible effect on the load-carrying capacity of corroded beams, especially on the ultimate load. However, the failure of the tested beams having high reductions of bond strength from 30% to 80% can occur earlier than that of the beam without bond strength reduction. For the tested beam FCL03 – 0, the applied load is suddenly reduced at the deflection of 9.0 mm in comparison with approximately 4.2 mm on the other.

b. Effect of the cross-section loss

Fig. 14 shows the simulation results of the load – deflection curves of the tested beams with the cross-sectional tension reinforcement loss ranging from 10% to 50%. It can be seen that the effect of the cross-section loss on the flexural carrying capacity of tested beams is more significant than the reduction of bond strength. The load-carrying capacity of tested beams is reduced by increasing the cross-section loss of tension reinforcement. As an example, the ultimate load of the tested beams decreases by 40% when the cross-section loss raises from 0% to 30% (100 kN on the beam FCL03–0 versus 60 kN on the beam FCL03–2). This decrease of the ultimate load can be up to more than 60% with the 50% cross-section loss. Moreover, the deflection at the middle span is greatly reduced on the beam FCL03-3. The failure mode of the tested beams shifted from ductile to brittle fracture with an important cross-section loss. This type of brittle failure can be predicted with the FE simulation.

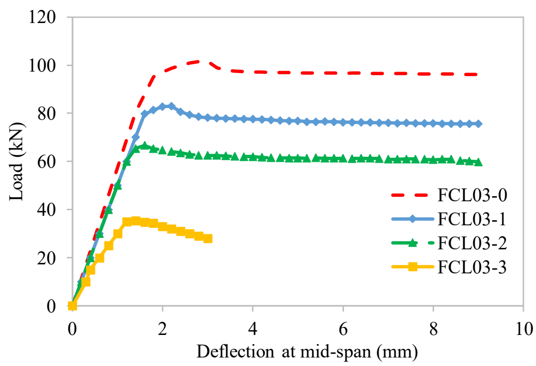

Figure 14. Load - deflection curves with several cross-section losses

4. Conclusions

In this paper, the effects of the stirrup corrosion on the flexural capacity of five corroded RC beams have been simulated and discussed. FE analysis method with DIANA software has been provided to simulate the structural responses of the corroded beams to consider two different inputs: (i) without stirrups in flexural span, (ii) with corroded stirrups at different locations. The validation of the FE model is presented by comparing the numerical and experimental results of the load – deflection curves. A parametric simulation was also realized to assess the effect of the bond strength reduction and the cross-section loss of tension reinforcements on the flexural capacity of the corroded beam. The obtained results allow us to draw the main conclusions as follows:

- The FE model that was adopted in this paper provides a good prediction of the flexural capacity (e.g. load carrying capacity, load – deflection curve) of the corroded beams by modeling the corrosion damage on the reinforcement, concrete and steel – concrete bond.

- The FEM analysis can detect the impact of stirrups corrosion on the flexural behavior of the corroded beam by representing the reduction of the deflection at the middle span. For a corroded beam with local corroded stirrups, severe corrosion of approximately 30% weight loss for the stirrup in the shear span can be a good example. On the other hand, there is no significant change in terms of both flexural capacity and ductility in corroded beams compared with the control beam by only applying uniform corrosion in U-type stirrup.

- While in the design stage of a structure, engineers do not often consider the influence of stirrups in the flexural capacity of the beam. However, the obtained results show that the stirrups corrosion should receive more attention in the serviceability limit state due to its considerable effect on flexural capacity, induced reduction of stiffness and ductility of existing reinforced concrete beam.

- The effect of the cross-section loss of tension reinforcements on the flexural capacity of the corroded beam (e.g. ultimate load, deflection) is more significant than the bond strength reduction. The failure mode of the corroded beam can be changed from ductile to brittle fracture with an important cross-section loss.

References

[1] Lim, S., Akiyama, M., Frangopol, D. M. (2016). Assessment of the structural performance of corrosion-affected RC members based on experimental study and probabilistic modeling. *Engineering Structures*, 127:189–205.

[2] Coronelli, D., Gambarova, P. (2004). Structural Assessment of Corroded Reinforced Concrete Beams: Modeling Guidelines. *Journal of Structural Engineering*, 130(8):1214–1224.

[3] Kallias, A. N., Rafiq, M. I. (2010). Finite element investigation of the structural response of corroded RC beams. *Engineering Structures*, 32(9):2984–2994.

[4] Sæther, I., Sand, B. (2012). FEM simulations of reinforced concrete beams attacked by corrosion. *ACI Structural Journal*, 109(2):15–31.

[5] Hai, D. T., Yamada, H., Katsuchi, H. (2007). Present condition of highway bridges in Vietnam: an analysis of current failure modes and their main causes. *Structure and Infrastructure Engineering*, 3(1):61–73.

[6] Tan, N. N., Hiep, D. V. (2020). Empirical models of corrosion rate prediction of steel in reinforced concrete structures. *Journal of Science and Technology in Civil Engineering (STCE)-NUCE*, 14(2):98–107.

[7] Tan, N. N., Dung, T. A., The, N. C., Tuan, T. B., Anh, L. T. (2018). An experimental study to identify the influence of reinforcement corrosion on steel-concrete bond stress. *Journal of Science and Technology in Civil Engineering (STCE)-NUCE*, 12(6):29–38. (in Vietnamese).

[8] Nguyen, N. D., Tan, N. N. (2019). Prediction of residual carrying capacity of RC column subjected in-plane axial load considering corroded longitudinal steel bars. *Journal of Science and Technology in Civil Engineering (STCE)-NUCE*, 13(2V):53–62. (in Vietnamese).

[9] Capé, M. (1999). Residual service-life assessment of existing R/C structures. Master's thesis, Gothenburg, Sweden: Chalmers University of Technology, and Milan, Italy: Milan University of Technology.

[10] Molina, F. J., Alonso, C., Andrade, C. (1993). Cover cracking as a function of rebar corrosion: Part 2—Numerical model. *Materials and Structures*, 26(9):532–548.

[11] Val, D. V. (2007). Deterioration of Strength of RC Beams due to Corrosion and Its Influence on Beam Reliability. *Journal of Structural Engineering*, 133(9):1297–1306.

[12] Du, Y. G., Clark, L. A., Chan, A. H. C. (2005). Residual capacity of corroded reinforcing bars. *Magazine of Concrete Research*, 57(3):135–147.

[13] CEB-FIP Model Code (1990). *Design code*. Thomas Telford, London.

[14] Dong, J., Zhao, Y., Wang, K., Jin, W. (2017). Crack propagation and flexural behaviour of RC beams under simultaneous sustained loading and steel corrosion. *Construction and Building Materials*, 151: 208–219.

[15] Ullah, R., Yokota, H., Hashimoto, K., Goto, S. (2016). Load carrying capacity of RC beams with locally corroded shear reinforcement. *Journal of Asian Concrete Federation*, 2(1):46.